Downregulation of miR-223 Expression Is an Early Event during Mammary Transformation and Confers Resistance to CDK4/6 Inhibitors in Luminal Breast Cancer

Francesca Citron[1], Ilenia Segatto[1], Gian Luca Rampioni Vinciguerra[1,2], Lorena Musco[1], Francesca Russo[1], Giorgia Mungo[1], Sara D'Andrea[1], Maria Chiara Mattevi[1], Tiziana Perin[3], Monica Schiappacassi[1], Samuele Massarut[4], Cristina Marchini[5], Augusto Amici[5], Andrea Vecchione[2], Gustavo Baldassarre[1], and Barbara Belletti[1]

ABSTRACT

miR-223 is an anti-inflammatory miRNA that in cancer acts either as an oncosuppressor or oncopromoter, in a context-dependent manner. In breast cancer, we demonstrated that it dampens the activation of the EGF pathway. However, little is known on the role of miR-223 during breast cancer onset and progression. miR-223 expression was decreased in breast cancer of luminal and HER2 subtypes and inversely correlated with patients' prognosis. In normal luminal mammary epithelial cells, miR-223 acted cell autonomously in the control of their growth and morphology in three-dimensional context. In the MMTV-Δ16HER2 transgenic mouse model, oncogene transformation resulted in a timely abrogation of miR-223 expression, likely due to activation of E2F1, a known repressor of miR-223 transcription. Accordingly, treatment with CDK4/6 inhibitors, which eventually results in restraining E2F1 activity, restored miR-223 expression and miR-223 ablation induced luminal breast cancer resistance to CDK4/6 inhibition, both *in vitro* and *in vivo*. Notably, miR-223 expression was lost in microdissected ductal carcinoma *in situ* (DCIS) from patients with luminal and HER2-positive breast cancer. Altogether, these results identify downmodulation of miR-223 as an early step in luminal breast cancer onset and suggest that it could be used to identify aggressive DCIS and predict the response to targeted therapy.

Significance: miR-223 may represent a predictive biomarker of response to CDK4/6 inhibitors and its loss could identify DCIS lesions that are likely to progress into invasive breast cancer.

Introduction

MiRNAs are small noncoding RNAs that interact with specific target mRNAs, thereby causing their translational repression or degradation. miRNAs play important roles in many biological processes, at both physiologic and pathologic levels. In cancer, miRNAs can function either as oncogenes or tumor-suppressor genes, depending on the target(s) they regulate and from the tissue-specific context (1, 2).

Recently, we investigated the biological effects exerted by intraoperative radiotherapy (IORT) in the tumor microenvironment of patients with early breast cancer (3). To reduce the risk of recurrence, radiotherapy is used as a standard adjuvant treatment, and it is known that it exerts its functions by both killing residual tumor cells and altering the microenvironment. In the setting of IORT, we demonstrated that soon after the delivery of radiation, a local upregulation of miR-223 expression was observed in the breast peritumoral microenvironment. In this context, miR-223 targeted the EGF, attenuating its local release and the autocrine/paracrine EGF/EGFR signaling activation that was strongly induced by the surgical wound (3). The dampening of the EGFR pathway by miR-223 eventually resulted in decreased survival of residual isolated cancer cells, locally left behind after surgery, which, at least in part, translated into the improved recurrence-free survival observable in IORT-treated patients (4, 5).

Literature regarding miR-223 is mainly centered on its role in myelopoiesis (6, 7); however, several studies have highlighted its dysregulation in various diseases, including cancer (8). miR-223 expression is decreased in many different tumors, both hematologic and solid, inversely correlating with increased cancer cell growth, invasion, and chemoresistance (9–13). As only exceptions, esophageal and gastric cancers display a direct correlation between miR-223 and tumor aggressiveness (14, 15). Interestingly, in colon and breast cancer cells, gain-of-function mutants of p53 bind and downregulate miR-223 promoter activity, overall decreasing miR-223 expression and protecting cells from drug-induced cell death (9). Others and we also demonstrated that E2F1 binds to the miR-223 promoter and inhibits miR-223 transcription, suggesting that E2F1 could act as a transcriptional repressor of miR-223 gene (3, 12, 16). Altogether, different studies suggest that repression of miR-223 represents a general feature during cancer progression. However, no study has addressed the role of miR-223 during the first steps of mammary tumorigenesis. With the widespread use of screening mammography, ductal carcinoma *in situ* (DCIS), a precancerous mammary lesion, accounts for approximately 20% of all newly diagnosed breast carcinomas. Although virtually all

[1]Molecular Oncology Unit, Centro di Riferimento Oncologico di Aviano (CRO), IRCCS, National Cancer Institute, Aviano, Italy. [2]Faculty of Medicine and Psychology, Department of Clinical and Molecular Medicine, University of Rome "Sapienza" Sant'Andrea Hospital, Rome, Italy. [3]Pathology Unit, Centro di Riferimento Oncologico di Aviano (CRO), IRCCS, National Cancer Institute, Aviano, Italy. [4]Breast Surgery Unit, Centro di Riferimento Oncologico di Aviano (CRO), IRCCS, National Cancer Institute, Aviano, Italy. [5]Department of Biosciences and Veterinary Medicine, University of Camerino, Camerino, Italy.

Note: Supplementary data for this article are available at Cancer Research Online (http://cancerres.aacrjournals.org/).

Corresponding Authors: Barbara Belletti, Centro di Riferimento Oncologico di Aviano (CRO), IRCCS, National Cancer Institute, Via Gallini 2, Aviano 33081, Italy. Phone: 39-0434-659661; Fax: 39-0434-659428; E-mail bbelletti@cro.it; and Gustavo Baldassarre, Phone: 30-0434-659759; E-mail gbaldassarre@cro.it

Cancer Res 2020;80:1064–77

doi: 10.1158/0008-5472.CAN-19-1793

invasive cancer begins as DCIS, not all DCIS will become invasive cancer (17). It is estimated that only about 20% to 30% of women with DCIS who do not receive treatment will develop breast cancer. Up to now, there is no definite way of determining which lesions will remain stable without treatment and which will go on to become invasive. Therefore, almost all women with DCIS will be treated.

Here, by investigating the role of miR-223 in mammary epithelial cells during mammary tumorigenesis, we highlight that loss of miR-223 is an early event during breast transformation and suggest that the evaluation of its expression could serve as prognostic factor in DCIS and predict the response to specific targeted therapies.

Materials and Methods

Study approval and primary tumor collection

Primary breast cancer specimens were collected from patients with breast cancer upon signing a written informed consent, in accordance with recognized ethical guidelines and following approval by the Institutional Review Board of CRO Aviano, National Cancer Institute (Aviano, Italy) and University of Rome "Sapienza" Santo Andrea Hospital (Rome, Italy). Breast cancer specimens were immediately frozen and stored at −80°C or formalin fixed, as appropriate.

Animal experimentation

Animal experimentation was approved by the Italian Ministry of Health (#616/2015-PR) and by our Institutional Animal Care and Use Committee (OPBA) and conducted strictly complying with internationally accepted guidelines (IACUC) for animal research and with the 3Rs principles.

FVB miR-223 knockout mice (miR-223 KO) were housed and bred as previously described (3). MMTV-Δ16HER2 mice were generated and characterized (18) and housed in our animal facility. FVB-MMTV-Δ16HER2 mice and FVB-miR-223 KO mice were crossed to generate FVB MMTV-Δ16HER2 miR-223 KO mouse colony. Experimental details and protocols can be found in Supplementary Data.

Cell culture, transfection, and generation of stable cell clones

BPE-3 cells (hereafter BPEC) were purchased from LTCC (Live Tissue Culture Service Center-LTCC@med.miami.edu) and grown in BMI-P medium (LTCC), supplemented with cholera toxin 100 ng/mL (Sigma), as previously published (19, 20) and strictly following all the manufacturer's instructions. Normal murine mammary gland (NMuMG) cells were a kind gift of Dr. Andrei V. Bakin at Roswell Park Comprehensive Cancer Center (Buffalo, NY; ref. 21) and grown in DMEM (Sigma) supplemented with 10% FBS (Carlo Erba). All other cell lines were obtained from the ATCC, maintained in culture following the ATCC indications, and grown in standard conditions at 37°C and 5% CO_2. Human cell lines were authenticated by short tandem repeat (STR) analysis in 2018, according to PowerPlex 16 HS System (Promega) protocol and using GeneMapper software 5 (Thermo Fisher) to identify DNA STR profiles and routinely tested to exclude Mycoplasma contamination (MycoAlert, Lonza). BPEC, HMEC, and NMuMG cells were expanded and frozen immediately into numerous aliquots immediately after their arrival. Cells revived from the frozen stock were then used for 4 to 6 passages and, however, not exceeding a period of 1 month. BPEC, NMuMG, and MCF7 cells were transfected with pcDNA3CMV His-Tag empty vector (Control), or with pcDNA3CMV HER2^{WT}, pcDNA3CMV HER2^{V659E} (Addgene #16257 and #16259), pcDNA3CMV Δ16HER2 (18), pEGFP KRas^{G12D} (22), pEGFP TP53^{R273H} (23), pcDNA PI3K WT, or H1047R (Addgene plasmids # 16643 and #16639) expression vectors. Experimental details and protocols can be found in Supplementary Data.

Three-dimensional mammary epithelial cell cultures and colony assay

Three-dimensional (3D) cell culture was performed as previously described (22). For colony assay, BPEC cells modified for miR-223 levels, overexpressing or not the different isoforms of HER2, were trypsinized, counted, and seeded at density 2×10^3 cells/well of a 6-well plate and incubated in complete medium. After 2 weeks, plates were stained with crystal violet, and colonies were manually counted, as previously described (24, 25). Experimental details and protocols can be found in Supplementary Data.

Cell viability and kill curve with palbociclib

For growth curve analyses, BPEC control or antimiR-223 cells were seeded in 96-well culture plates (2×10^3 cells/well), and after 24 hours, cell proliferation was measured with CellTiter 96 AQueous One Solution Cell Proliferation (MTS) Assay (Promega) every day for 6 consecutive days, as previously described (26). For kill curve, BPEC and MCF7 cells were seeded in 96-well culture plates (4×10^3 cells/well). After 24 hours, cells were treated with increasing doses of palbociclib - PD-0332991 hydrochloride (Clinisciences), as indicated. Experimental details and protocols can be found in Supplementary Data.

Histologic analysis and immunofluorescence

Dissected abdominal mammary glands or tumors were fixed in formalin and processed for standard embedding in paraffin. Histologic sections (5 μm thick) were cut from the paraffin blocks, deparaffinized with xylene, and stained with hematoxylin and eosin, according to standard procedures.

Immunofluorescence analyses on mammary acini grown in 3D culture were performed as previously described (3, 20). Samples were analyzed using a confocal laser-scanning microscope (TSP8, Leica) interfaced with a Leica fluorescent microscope. Collected images were analyzed using the LAS (Leica) and the Volocity (PerkinElmer) softwares. Experimental details and protocols can be found in Supplementary Data.

Quantitative real-time PCR and digital droplet PCR

RNA from mammary tissue or cells was extracted using TRIzol reagent (Invitrogen, Thermo Fisher Scientific). Disruption of the tissue sample was achieved by using the GentleMACS Dissociator (Miltenyi Biotec) and by passing the lysate at least 5 times through a 23-gauge needle fitted to an RNase-free syringe. Total RNA was quantified using the QuantiFluor RNA System (Promega). RNA was retrotranscribed using the GoScript Reverse Transcriptase (Promega), and retrotranscribed reactions were run in an Opticon qRT-PCR Thermocycler (Bio-Rad).

In microdissected tissues, expression of miR-223, miR-484, miR-1257, miR-9, and U6 was evaluated using digital droplet PCR (ddPCR) analysis. First, areas of normal tissue, DCIS, or invasive ductal carcinoma (IDC) were microdissected from each of the 14 breast cancer samples. Total RNA from microdissected samples was extracted using TRIzol reagent (Invitrogen) and quantified using QuantiFluor RNA System (Promega). Before droplets generation, ddPCR reactions were prepared in similarly qRT-PCR reactions, following the manufacturer's instructions. Briefly, 0.2 ng RNA equivalent of cDNA was mixed with ddPCR Supermix for Probes (No dUTP) 2x (Bio-Rad) and the appropriate Taqman probes (Thermo Fisher Scientific). Within each sample, we evaluated the expression of miR-223, U6, and four other unrelated miRNAs and used their mean value to normalize miR-223 expression (Thermo Fisher Scientific, hsa-miR-223 #002295; hsa-miR-34a #000426; hsa-miR-484 #001821; hsa-miR-1257 #002910; hsa-miR-9-1-5p #000583; U6 snRNA #001973).

The droplet generation was performed in a QX200 Droplet Generator (Bio-Rad) using Droplet Generation Oil for Probes (Bio-Rad), according to the manufacturer's protocol. miRNA absolute quantification was achieved using QX200 Droplet Reader (Bio-Rad) and data analyzed with QuantaSoft (Bio-Rad).

Preparation of protein lysates and Western blot analysis

Protein lysates and Western blot were performed essentially as previously described (22, 26–28). Experimental details and protocols can be found in Supplementary Data.

Statistical analyses and reproducibility

Statistical significance, means, median, and SD were determined by using GraphPad PRISM software (version 6.01), using the most appropriate test, as specified in each figure. A minimum of three biologically independent experiments was used for statistical significance. The number and type of replicates used in each experiment are specified in the figure legends. When not otherwise specified, mean and SD are shown in all graphs. Significance was calculated by the Student *t* test or Mann–Whitney two-sided test or ANOVA, as appropriate, and indicated by a $P < 0.05$.

Kaplan–Meier survival curves were generated using the KM Plotter online tool (http://kmplot.com), using the most appropriate cutoff value. KM Plotter is an online algorithm exploitable to interrogate the expression of up to 54,675 genes in up to 3,951 patients with breast cancer, with a mean follow up of 40 months. The miRNA subsystems include 11k samples from 20 different cancer types. Primary purpose of the tool is a meta-analysis–based discovery and validation of survival biomarkers (29).

Results

miR-223 expression levels inversely correlate with survival in patients with breast cancer

Recently, we found that miR-223 was upregulated in human mammary gland following administration of IORT and, by targeting the EGF, resulted in dampening of auto/paracrine EGF/EGFR signaling activation (3). Moreover, we observed that in The Cancer Genome Atlas dataset, miR-223 expression was decreased in malignant breast tumors, particularly in the luminal and HER2 subtypes (16). We thus interrogated several datasets containing clinical information, to evaluate whether the decreased expression level of miR-223 could also have pathologic implications. In all datasets, the analysis of miR-223 in correlation with patients' prognosis clearly indicated that low miR-223 levels correlated with reduced overall survival and worse prognosis (**Fig. 1A** and **B**).

miR-223 expression is reduced in breast cancer samples and cell lines compared with normal counterparts

Based on these *in silico* results, we analyzed miR-223 expression in an internal cohort of breast cancer specimens (147 primary tumors and 36 normal adjacent breast tissues, taken at least 2 cm from tumor; Supplementary Table S1) and in a large panel of breast cancer cell lines, encompassing the main breast cancer subtypes (hormone receptor–positive, luminal; HER2 enriched, luminal or basal; triple negative). By this analysis, we confirmed the *in silico* data and showed that miR-223 expression was reduced in breast cancer respect to the normal mammary tissue, especially in the luminal and HER2 luminal subtypes (**Fig. 1C**). Accordingly, analysis of miR-223 expression in breast cancer and matched normal adjacent tissue from the same patient clearly showed that miR-223 was strongly decreased in the tumor compared with the healthy counterpart, and, again, this was particularly evident in luminal and HER2 luminal breast cancer (**Fig. 1D**).

In line with the results obtained in primary tumor samples, substantially all transformed breast cancer cell lines displayed decreased levels of miR-223 expression compared with normal epithelial (HMEC and BPEC) or benign fibroadenoma (MCF12A and MCF10A) cell lines (**Fig. 1E**). Only NMuMG cells were in contrast with this tendency and, although nontransformed, displayed very low levels of miR-223 expression (**Fig. 1E**). Among breast cancer cell lines, those derived from triple-negative breast cancer expressed the highest levels of miR-223, again recapitulating what observed in human samples.

These results supported the conclusion that miR-223 is well expressed in normal mammary epithelial cells and is downmodulated in breast cancer, especially if the luminal subtype is considered.

miR-223 expression levels critically control the growth of normal mammary epithelial cells

We thus decided to investigate further the role of miR-223 in mammary epithelial cells and its regulation during transformation. To this aim, we manipulated normal breast primary epithelial cells of the luminal subtype (BPEC) to stably knockdown miR-223 expression (**Fig. 2A**) and characterized their growth behavior in two-dimensional (2D) and in 3D context. Together with previous results collected in normal breast primary epithelial cells of the basal-type (HMEC; ref. 3), our present data confirmed that knocking down miR-223 expression in normal mammary epithelial cells enhanced cell proliferation (**Fig. 2B–F**) and led to hyperactivation of EGFR (pY1068) in 2D culture and in 3D Matrigel (**Fig. 2G–I**). Looking at cell morphology, miR-223 levels also affected the 3D organization of mammary acini in Matrigel. BPEC cells in which miR-223 expression was abrogated (anti–miR-223) formed more numerous, bigger, and more disorganized colonies (**Fig. 2D**). Conversely, in MCF7 luminal breast cancer cells, which endogenously express very low levels of miR-223 (**Fig. 1E**), overexpression of miR-223 not only induced formation of colonies that were less in number and smaller in size (**Fig. 2J–L**) as previously reported also for HER2-overexpressing BT-474 cells (3), but also the reacquisition of the regular structure of a mammary acini (**Fig. 2L**). In particular, apicobasal polarity was partially regained, as shown by restoration of apical tight junction (ZO-1), adherens junctions (β-catenin), and, in some cases, by the formation of hollow lumens (**Fig. 2L**).

Knockout of miR-223 marginally affects murine mammary gland development and Δ16HER2-driven tumorigenesis

Data collected so far indicated a possible role for miR-223 in the regulation of normal and tumor-derived breast epithelial cells. In our previous study, we found that, in human mammary gland microenvironment, miR-223 regulated EGF levels (3) that represent a key growth factor in mammary gland postnatal development. We thus tested *in vivo* if miR-223 was necessary for proper mammary gland postnatal development.

First, we evaluated the role of miR-223 and the effect of its depletion in NMuMG development (3, 6) In WT mice, there was a striking inverse correlation between miR-223 expression levels and the developmental stage of the gland, showing that the expansion of the mammary epithelial cell compartment during pregnancy corresponded to gradually reduced miR-223 levels and reaching its lowest level one day postpartum, when the mouse mammary glands (MMG) is fully developed and ready for lactation (**Fig. 3A**, top plots; **Fig. 3B** and **C**). However, the KO of miR-223 gene did not significantly affect mammary gland postnatal development (**Fig. 3A**, bottom plots;

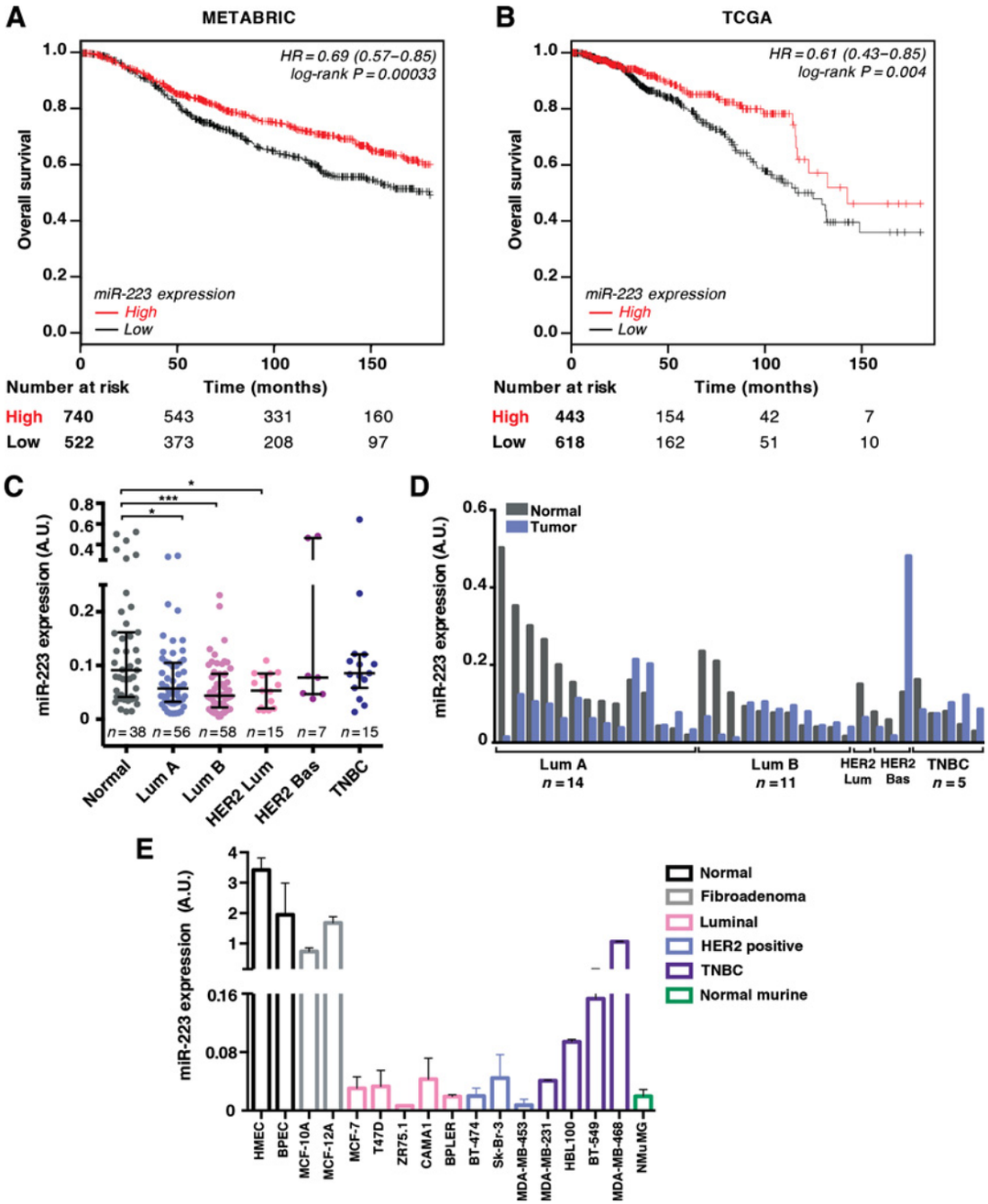

Figure 1.

miR-223 expression is reduced in breast cancer samples and inversely correlates with survival of patients with breast cancer. **A,** Kaplan–Meier survival curve evaluating the overall survival of patients with breast cancer, based on the expression of miR-223, using the KM Plotter online tool in the Metabric dataset ($n = 1{,}262$). **B,** Same as in **A**, in The Cancer Genome Atlas (TCGA) dataset ($n = 1{,}061$). **C,** Graph reports the data from qRT-PCR analysis of normalized miR-223 expression in normal mammary gland and breast cancer tissues of different subtypes, as indicated. The median value with range is reported. Significance was calculated using the Mann–Whitney test. **D,** Graph reports the data from qRT-PCR analysis of normalized miR-223 expression in matched normal and breast cancer samples of different subtypes, as indicated. **E,** Graph reports the data from qRT-PCR analysis of normalized miR-223 expression in a panel of mammary epithelial cell lines, normal, benign, or malignant of the different subtypes, as indicated. When not otherwise specified, in all graphs, data represent the mean value (± SD) of three independent assays performed in duplicates and are expressed as arbitrary units (A.U.). Asterisks indicate significant differences. *, $P \leq 0.05$; ***, $P \leq 0.001$.

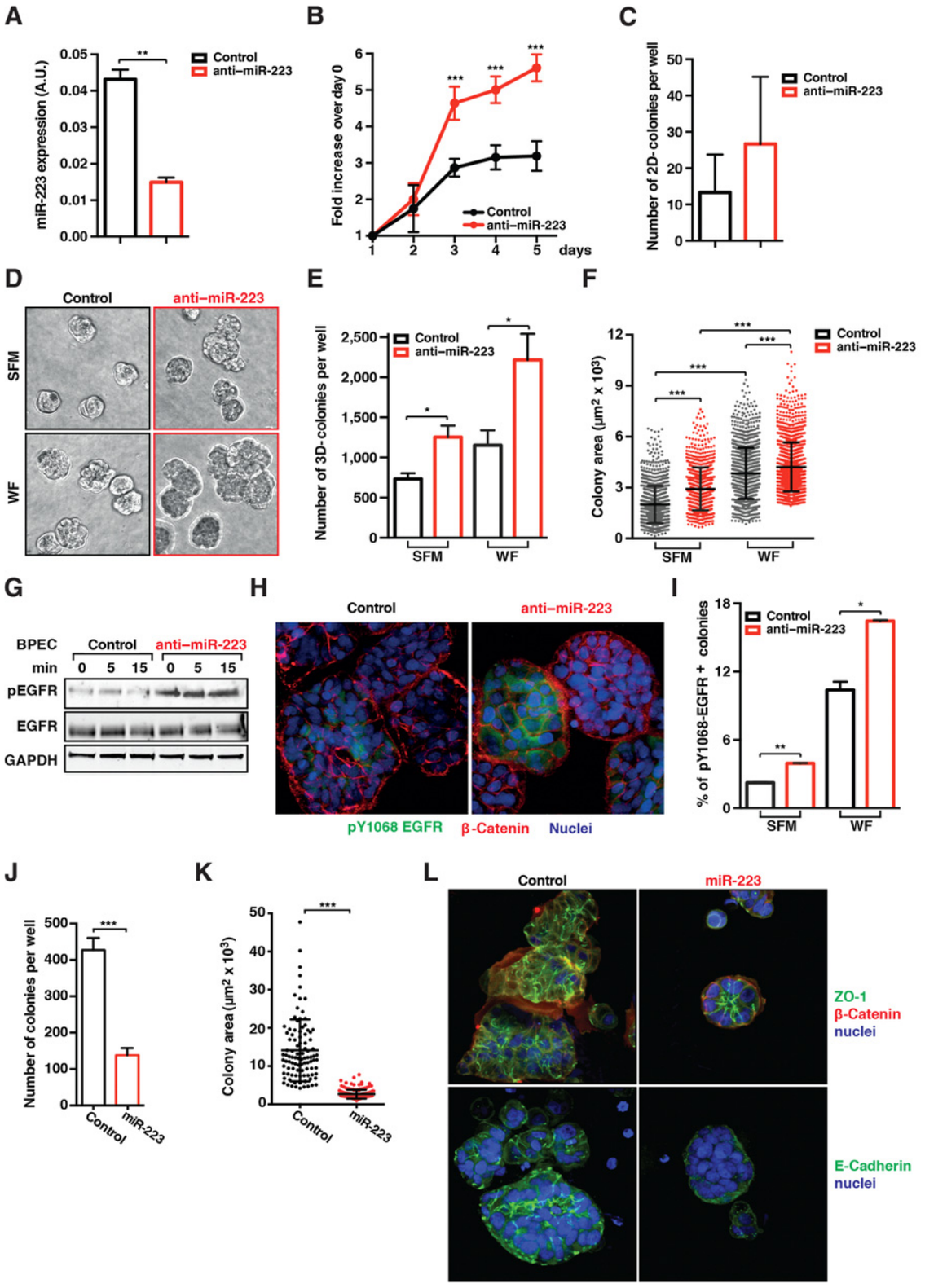

Supplementary Fig. S1A and S1B). Accordingly, female miR-223 KO mice properly lactated their litter, suggesting that compensating mechanisms made up for the absence of miR-223 *in vivo*.

Next, to evaluate the effect of miR-223 loss in onset and progression of breast cancer, we crossbred miR-223 WT and KO mice with the Δ16HER2 transgenic mouse model, expressing an HER2 splicing variant lacking a 16 aminoacids in the juxtamembrane domain and developing several aggressive mammary carcinomas, with 100% penetrance at approximately 15 weeks of age (18, 20). First, we fully characterized the new mouse colony in terms of tumor onset, latency, growth, number, and burden. With our surprise, genetic deletion of miR-223 did not affect in a significant manner any of the above-mentioned parameters (Supplementary Fig. S2A–S2F), although a slight tendency in increased number of foci and anticipation of tumor onset was detectable (Supplementary Fig. S2A and S2B). We also performed syngeneic injections of Δ16HER2 mammary epithelial cells (Δ16HER2 mMECs) using different donor–recipient combinations. We collected Δ16HER2 mMECs from tumors developed in miR-223 WT or KO mice and injected them into nontransgenic recipient mice, either miR-223 WT or KO. However, even in this setting, we did not observe any significant difference in tumor onset and growth among the different combinations, suggesting that KO of miR-223, either in the epithelial or in the stromal counterpart, did not significantly affect Δ16HER2-driven breast tumorigenesis (Supplementary Fig. S3A and S3B).

miR-223 is mainly expressed by the epithelial cell compartment of normal mammary tissue and is not expressed in Δ16HER2 tumors

These *in vivo* results were quite in contrast with our *in vitro* findings and with the observations made in human breast cancer samples (**Figs. 1** and **2**). We decided to evaluate which cell population was actually expressing miR-223 in the mammary gland. First, we performed ISH for miR-223, but we could not collect solid data regarding the specificity of the miR-223 probe using the miR-223 KO as negative control. Therefore, we performed tissue separation from the normal mouse mammary gland to enrich the epithelial versus the fibroblastic components and measured miR-223 levels in these two cell compartments. The results univocally indicated that the epithelial cells were the main contributors of miR-223 within the mammary gland (**Fig. 3D**). Then, we analyzed the pattern of Δ16HER2 oncogene activation and, in parallel, miR-223 expression in Δ16HER2-positive mice. In MMGs collected at 10 weeks of age, only few sparse cells (if any) expressed Δ16HER2; at 13 weeks of age, when we first start to observe the formation of tumor foci, there was an increase in Δ16HER2; finally, at 16 weeks of age, when large parts of the MMG are substituted by transformed cells, and at 20 weeks of age, when tumor masses have totally replaced the MMG, all cells become massively and intensely positive for Δ16HER2 (**Fig. 3E**). The parallel analysis of miR-223 showed that although it was readily expressed by the Δ16HER2 MMG in preneoplastic setting (10 weeks of age), it was completely lost in Δ16HER2 tumors and, accordingly, in the epithelial cell population extracted from the tumor (**Fig. 3F**). Thus, once that the oncogene was activated, Δ16HER2-positive mMECs from miR-223 WT mice became substantially knocked out for miR-223 expression, indirectly clarifying why we did not detect any difference in tumor phenotypes in miR-223 KO compared with WT animals (Supplementary Figs. S3 and S4).

miR-223 expression partially controls HER2-driven breast cancer cell proliferation and 3D organization

To confirm these data in a more controlled *in vitro* system, we knocked down miR-223 expression (anti–miR-223) in normal epithelial cells of basal (HMEC) and luminal (BPEC) subtype and transformed them with different HER2 isoforms, namely the WT, the Δ16HER2, and the $HER2^{V659E}$, a variant carrying a mutation in the juxtamembrane domain (**Fig. 4A**; Supplementary Fig. S4A; refs. 30, 31).

Down modulation of miR-223 expression (anti–miR-223) increased the 3D growth in control BPEC (**Fig. 4B–D**), as already observed in HMEC (Supplementary Fig. S4; ref. 3). As expected, all isoforms of HER2 significantly stimulated the 3D Matrigel growth, both in control BPEC and HMEC (**Fig. 4B–D**; Supplementary Fig. S4B and S4C). However, the expression of the constitutively active isoforms of HER2 did not add a significant 3D-growth advantage in cells that were already downmodulated for miR-223 (anti–miR-223 empty), suggesting that they acted on the same signaling axis (**Fig. 4B–D**; Supplementary Fig. S4B and S4C). A closer look to $HER2^{WT}$-expressing cells demonstrated that miR-223 downmodulation resulted in increased proliferation, as evidenced by the higher number of Ki67-positive cells in colonies from anti–miR-223 HMEC (Supplementary Fig. S4D and S4E). We also observed that $HER2^{WT}$-expressing MCF7 and NMuMG cells remained sensitive to EGF stimulation for their growth, while they become EGF insensitive if expressing Δ16HER2 (**Fig. 4E** and **F**). Overall, these data indicate that miR-223 participates to the control of breast cancer cell proliferation, in part by regulating the expression of EGF. But when HER2 is constitutively activated (Δ16HER2), the possible contribution of miR-223 silencing and/or EGF to the transformed phenotype is lost.

miR-223 expression is rapidly downmodulated following cell transformation

Many data that we collected both *in vitro* and *in vivo* described an inverse correlation between miR-223 expression and cell

Figure 2.

Downmodulation of miR-223 expression levels alters the growth of mammary epithelial cells. **A,** Graph reports the data from qRT-PCR analysis of normalized miR-223 expression (in arbitrary units, A.U.) in BPEC cells stably transduced with control and anti–miR-223 lentiviral vectors. **B,** Graph reports the data from growth curve analysis of control and anti–miR-223 BPEC cells, expressed as fold increase over the number of cells plated on day 0. Cell viability was measured every day for 5 days by MTS assay. **C,** Graph reports the data from clonogenic assay of control and anti–miR-223 BPEC cells. The total number of colonies/well after 15 days is reported. **D,** Representative contrast-phase images of control and anti–miR-223 BPEC cells included in 3D Matrigel, grown in serum-free media (SFM) supplemented or not with 5% wound fluid (WF) and allowed to grow for 8 days. **E,** Graph reports the colony number/well of the experiment described in **D**. **F,** Graph reports the colony area of the experiment described in **D** measured using the Volocity software and expressed as $\mu m^2 \times 10^3$. Each dot corresponds to one colony. **G,** Western blot analysis of the indicated proteins in lysates from control and anti–miR-223 BPEC cells. GAPDH was used as loading control. **H,** Representative confocal images of immunofluorescence analyses of mammary acini in 3D Matrigel from control and anti–miR-223 BPEC cells, immunostained for pY^{1068}EGFR (green), E-cadherin (red), and nuclei (TO-PRO-3, blue). **I,** Graph reports the percentage of pY^{1068}EGFR-positive/all colonies of the well, from the experiment described in **H**. **J,** Graph reports the number of mammary acini/well formed by control and miR-223–overexpressing MCF7 cells in 3D Matrigel, allowed to grow for 8 days. **K,** Graph reports the colony area of the experiment described in **J** measured using the Volocity software and expressed as $\mu m^2 \times 10^3$. Each dot corresponds to one colony. **L,** Representative confocal images of mammary acini of the experiment described in **J**, immunostained for ZO-1 (green; top plots), β-catenin (red; top plots), E-cadherin (red; bottom plots), and nuclei (TO-PRO-3, blue). In all graphs, data represent the mean (± SD) of three independent experiments performed in duplicates. Student *t* test or Mann–Whitney test was used for statistical analysis, as appropriate. Asterisks indicate significant differences. *, $P \leq 0.05$; **, $P \leq 0.01$; ***, $P \leq 0.001$.

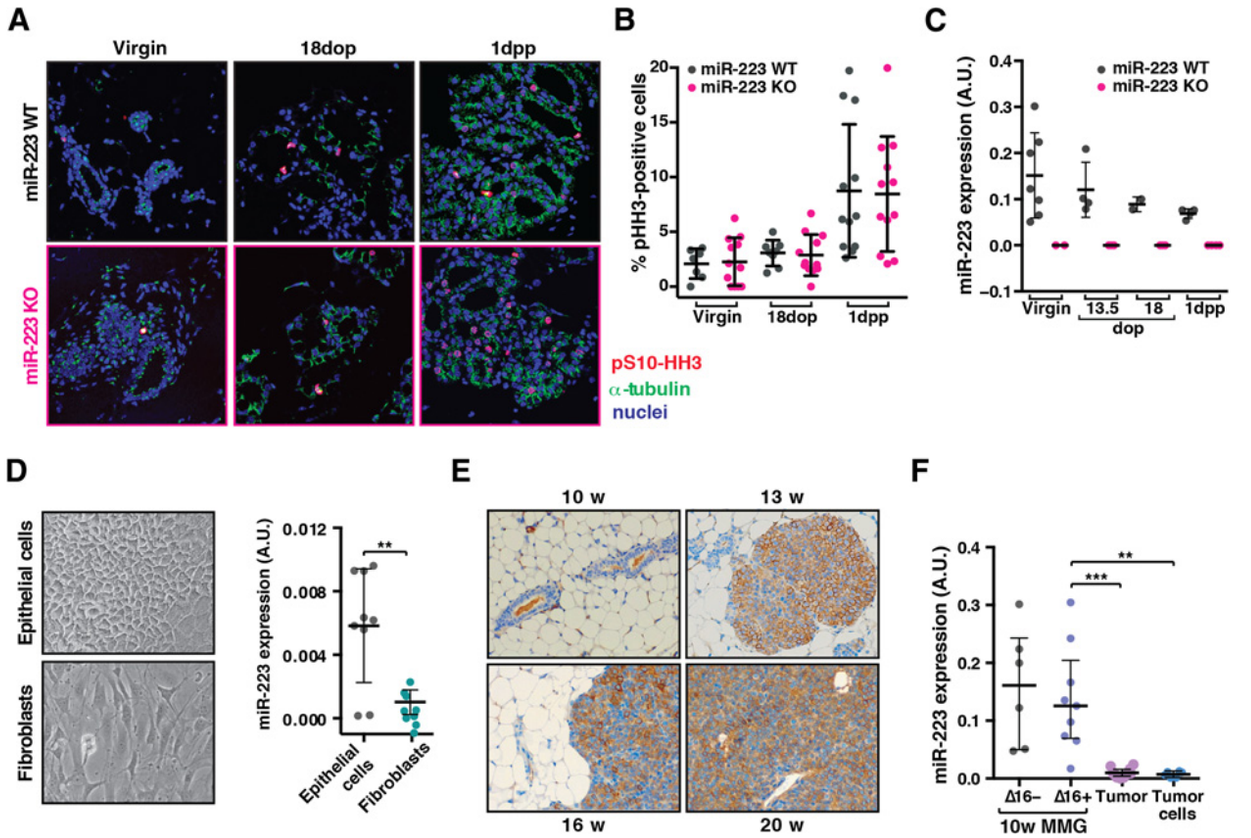

Figure 3.

miR-223 is expressed in the epithelial mammary cells, and its expression is rapidly downmodulated during tumorigenesis. **A,** Representative confocal images of MMGs immunostained for pS10-H3 (red), tubulin (green), and nuclei (TO-PRO-3, blue) and collected from miR-223 WT or KO female mice at different stages of development: 10-week virgin mice Δ16HER2 positive (Δ16+) and negative (Δ16-); 18 days of pregnancy (18 dop) and one day postpartum (1dpp) in Δ16- mice. **B,** Graph reports the quantification of pS10-H3–positive cells per field, from the MMGs described in **A**. **C,** Graph reports the data from qRT-PCR analysis of normalized miR-223 expression (in arbitrary units, A.U.) in MMGs described in **A**, plus the ones collected at 13.5 days of pregnancy (13.5 dop). Each dot represents a different MMG, and MMGs were collected from at least two different mice. **D,** Representative contrast-phase images of cell populations extracted from female MMG to separate the epithelial from the fibroblast counterpart (left plots). On the right, graph reports the data from qRT-PCR analysis of normalized miR-223 expression in the two indicated cell components. Each dot represents the cell extraction from a different mouse. **E,** Immunohistochemistry analysis of HER2 to detect Δ16HER2 transgene activation in MMG of Δ16HER2-positive female mice, collected at different time points (10-, 13-, 16-, and 20 weeks of age), as indicated. **F,** Graph reports the data from qRT-PCR analysis of normalized miR-223 expression (in arbitrary units, A.U.) in MMG from Δ16HER2-negative (Δ16-) or -positive (Δ16+) FVB female mice (10 weeks of age), in Δ16HER2 mammary tumors (20 weeks of age), and in tumor epithelial cells extracted from Δ16HER2+ mammary tumors. Each dot represents the miR-223 quantification in a different MMG, tumor, or cell preparation, as indicated in the graph. The Student *t* test was used for statistical analysis. Asterisks indicate significant differences. **, $P \leq 0.01$; ***, $P \leq 0.001$.

transformation and sustained proliferation. These results are in line with the notion that E2F1 is a strong transcriptional repressor of miR-223 promoter, and we already identified this as a mechanism contributing to unlock cell-cycle arrest (3, 16). Pulling together all this information, we hypothesized that the loss of miR-223 expression could represent a widespread and early event during cellular transformation, at least all times that E2F1 was directly or indirectly involved. To test this hypothesis, we transformed BPEC cells with different oncogenes and evaluated the expression of miR-233 before and after the expression of the oncogenic stimuli. As positive control, we used mutant TP53 that has been shown to downregulate miR-223 expression in cancer cells (9). After only 48 hours from oncogene transfection and expression (Supplementary Fig. S5A–S5D), we detected a consistent and significant decrease in miR-223 expression levels (**Fig. 5A**). In line with the data collected in 3D Matrigel, constitutively active forms of HER2 (Δ16 and V659E) were the oncogenes that more significantly decreased miR-223 levels in BPEC cells (**Fig. 5A**). Similar observations were obtained using the HMEC (Supplementary Fig. S5E) and NMuMG cells that, although expressing very low basal levels, decreased even further their miR-223 levels when transformed with different HER2 isoforms (Supplementary Fig. S5F and S5G).

miR-223 overexpression reduces the oncogenic potential of HER2-transformed mammary epithelial cells

Next, we asked if forcing miR-233 reexpression in tumor cells that have lost its expression could, at least partially, revert the transformed phenotype. We exploited NMuMG cells, which endogenously express very low levels of miR-223 (**Fig. 1E**), transformed them with Δ16HER2, and overexpressed miR-223 or a scramble sequence (control; **Fig. 5B**). Then, we orthotopically injected cells in the thoracic mammary fat pad (MFP) of athymic nude female mice and followed

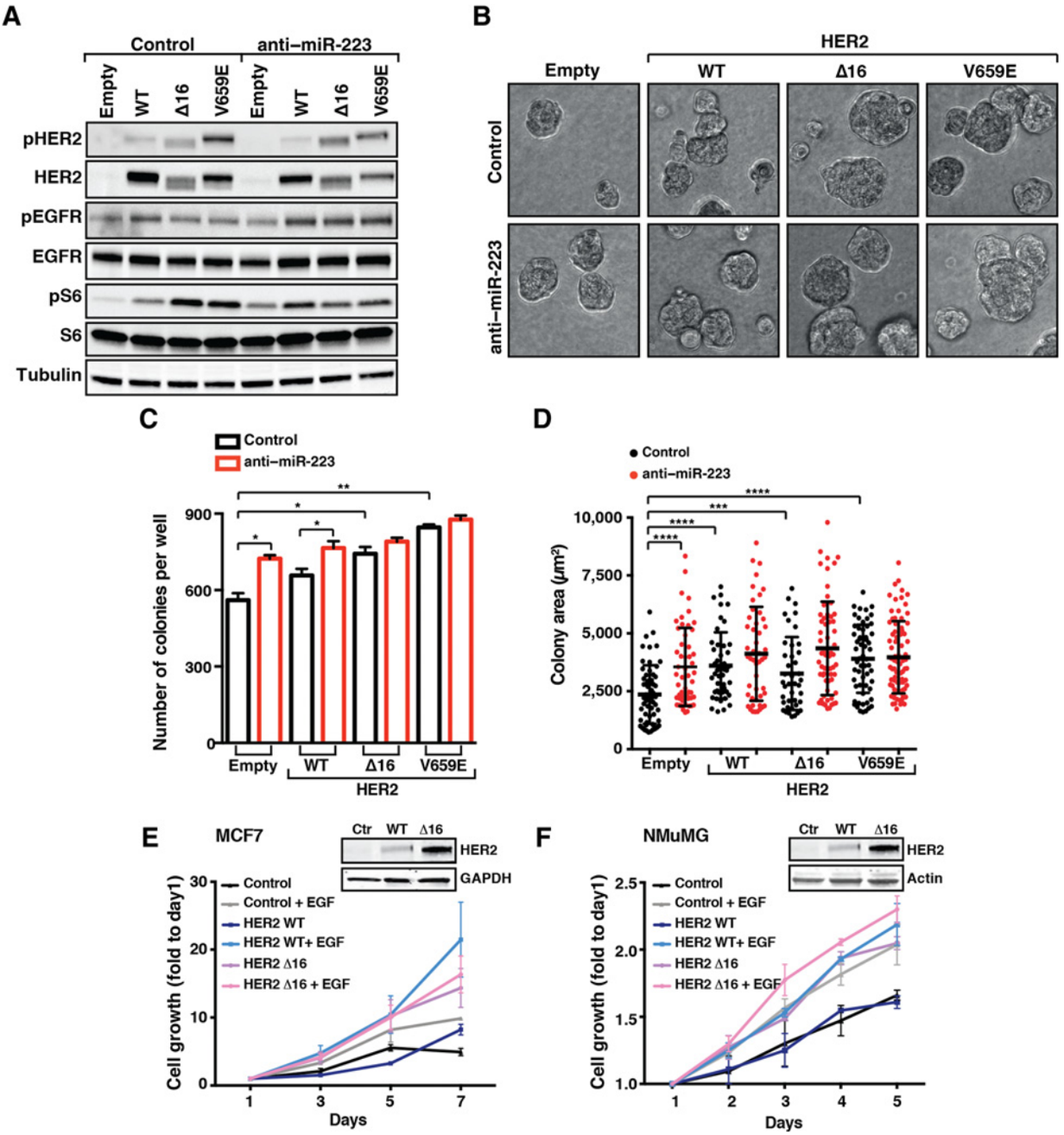

Figure 4.

miR-223 expression partially counteracts HER2-driven breast cancer cell proliferation and 3D organization. **A,** Western blot analysis of the indicated proteins in lysates from BPEC cells stably transduced with control or anti–miR-223 lentiviral vectors and transiently transfected with different HER2 isoforms (wild type, WT; Δ16HER2, Δ16; constitutively active, V659E) or empty vector, as indicated. Tubulin was used as loading control. **B,** Representative contrast-phase images of control and anti–miR-223 BPEC cells transiently transfected with empty vector or different HER2 isoforms (WT, Δ16, or V659E) included in 3D Matrigel and allowed to grow for 8 days. **C,** Graph reports the acini number/well of the experiment described in **B**. **D,** Graph reports the colony area of the experiment described in **B**, measured using the Volocity software and expressed as μm^2. Each dot corresponds to one colony. **E,** Growth curve analysis of MCF7 cells stably transfected with empty vector (Control) or different HER2 isoforms (WT and Δ16), as shown in the inset by Western blot analysis. GAPDH was used as loading control. Cells were plated at day 0 (50×10^3/well) in complete medium with or without the addition of EGF (20 ng/mL) and then counted by Trypan Blue exclusion test, every other day for 7 days. Data represents the mean (± SD) of two independent experiments performed in triplicate. **F,** Same as in **E**, but using NMuMG cells. *, $P \leq 0.05$; **, $P \leq 0.01$; ***, $P \leq 0.001$; ****, $P \leq 0.0001$.

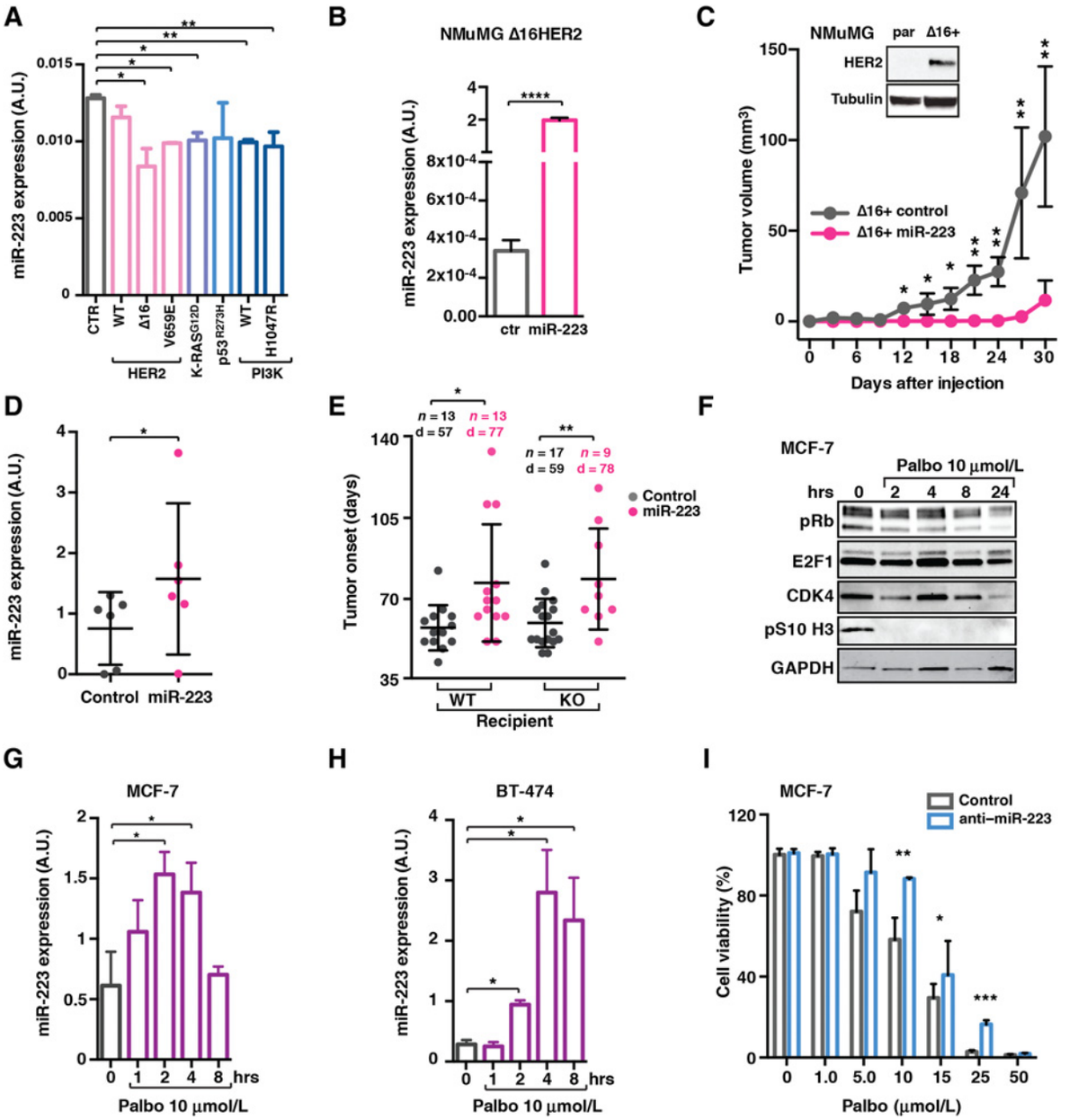

Figure 5.

miR-223 expression is rescued by antiproliferative stimuli and its overexpression reduces the oncogenic potential of HER2 in mammary epithelial cells. **A,** Graph reports the data from qRT-PCR analysis of normalized miR-223 expression (in arbitrary units, A.U.) in BPEC cells transiently transfected with an empty vector (CTR) or with vectors expressing the indicated oncogenes (HER2 WT, Δ16HER2, HER2^{V659E}, KRAS^{G12D}, TP53^{R273H}, PIK3CA WT, and PIK3CA^{H1074R}). Data of all graphs represent the mean (± SD) of three independent experiments performed in duplicates. **B,** Graph reports the data from qRT-PCR analysis of normalized miR-223 expression (in arbitrary units, A.U.) in NMuMG cells transfected with Δ16HER2 and stably transduced with control or miR-223–overexpressing vectors. **C,** Graph reports the tumor growth of Δ16HER2-NMuMG cells stably transduced with control or miR-223, injected in the MFP of athymic female nude mice. Tumor growth was monitored twice a week. Inset, the Western blot analysis of HER2 in lysates from parental and Δ16HER2+ NMuMG cells is reported. Tubulin was used as loading control. **D,** Graph reports the data from qRT-PCR analysis of normalized miR-223 expression in epithelial cells extracted from Δ16HER2- tumors transiently transduced with control or miR-223–overexpressing vectors. Each dot represents a different cell preparation. **E,** Graph reports the onset of tumors grown from Δ16HER2 epithelial cells, described in **D**, injected in the MFP of miR-223 WT or KO (Δ16HER2 negative) recipient mice. The number (*n*) of mice and the average time (days, d) of palpable tumor appearance are indicated at the top of each category. Each dot represents a different tumor. **F,** Western blot analysis of the indicated proteins in lysates from MCF7 parental cells treated with vehicle or palbociclib 10 μmol/L for the indicated time points (hours, hrs). GAPDH was used as loading control. **G** and **H,** Graphs report the data from qRT-PCR analysis of normalized miR-223 expression (in arbitrary units, A.U.) in MCF7 (**G**) and BT-474 (**H**) luminal breast cancer cell lines, treated with palbociclib 10 μmol/L for the indicated time points. **I,** Dose–response curve of MCF7 cells transiently transfected with control or anti–miR-223 oligo and treated for 72 hrs with increasing doses of palbociclib, as indicated. Cell viability was measured by MTS assay. Student *t* test was used for statistical analysis. Asterisks indicate significant differences. *, $P \leq 0.05$; **, $P \leq 0.01$; ***, $P \leq 0.001$; ****, $P \leq 0.0001$.

up xenografts' growth for 30 days. Overexpression of miR-223 drastically restrained Δ16HER2-driven tumor cell growth (**Fig. 5C**). To confirm these results in an immune-proficient model, we overexpressed miR-223 in mMECs extracted from Δ16HER2 tumors, which express very low levels of miR-223 (**Fig. 3F**), and then performed syngeneic injections in nontransgenic miR-223 WT or KO recipient mice. Again, miR-223 overexpression significantly delayed tumor onset, in line with what observed in nude mice (**Fig. 5D** and **E**). This experimental approach further suggested that miR-223 acted mainly in a cell-autonomous manner, because miR-223 overexpression in Δ16HER2 mMECs was able to delay tumor growth in both recipient mice genotypes (**Fig. 5E**).

miR-223 expression is a requisite for the response to CDK4/6 inhibition

We next reasoned that if transformation results in downregulation of miR-223, then pharmacologic treatments that impinge on E2F1 activity could rescue miR-223 expression. To this aim, we used the CDK4/6 inhibitor palbociclib, which, by reducing retinoblastoma (RB) phosphorylation, increases its binding to E2F1, thereby restraining its transcriptional activity and, eventually, blocking cell-cycle progression. We treated luminal (MCF7) and HER2 luminal (BT-474) breast cancer cells with palbociclib in a time course experiment and observed that miR-223 expression levels were increased following palbociclib treatment (**Fig. 5F–H**). The same was true also for Δ16HER2 mMECs that consistently increased miR-223 levels after palbociclib treatment (Supplementary Fig. S6A and S6B). To evaluate whether the upregulation of miR-223 was only a side effect or whether it was a necessary event for efficacy of the treatment, and we downmodulated miR-223 expression in MCF7 and in BPEC cells (anti–mir-223) before treating them with palbociclib. Following treatment, anti–miR-223 cells, unable to upregulate miR-223 expression, were significantly more resistant to palbociclib (**Fig. 5I**; Supplementary Fig. S6C).

Next, we asked whether miR-223 upregulation was also required to obtain a therapeutic response, *in vivo*. As a first approach, we extracted Δ16HER2 mMECs from miR-223 WT or KO tumors and orthotopically injected them in NSG mice or into syngeneic recipient miR-223 WT or KO mice. When tumors became palpable, we started to treat mice with palbociclib and followed tumor growth over time. In both experimental conditions, miR-223 WT Δ16HER2 tumors stopped their growth and also partially regressed, whereas corresponding tumors from miR-223 KO Δ16HER2 cells, which could not upregulate miR-223 following treatment, were resistant to palbociclib treatment and continued to grow (**Fig. 6A** and **B**). Then, we tested the response to palbociclib in Δ16HER2 transgenic miR-223 WT or KO mice that spontaneously develop multiple tumors in all MMG (Supplementary Fig. S2; refs. 18, 20). When first tumors became palpable, we started treatment with palbociclib for 8 weeks. After a transitory cytostatic effect, miR-223 KO tumors restarted to grow, whereas WT ones remained blocked at long term (**Fig. 6C**). More strikingly, the number of new tumors appearing under palbociclib treatment was dramatically higher in Δ16HER2 miR-223 KO mice compared with WT ones, indicating that palbociclib was highly effective in blocking the evolution of very small foci into frank tumors, but only when miR-223 could be upregulated (**Fig. 6D**). Altogether, the data collected strongly point to miR-223 as an important player in the response to CDK4/6 inhibition in Δ16HER2 breast cancer.

Loss of miR-223 is an early marker for mammary DCIS

Overall, the data collected *in vitro* and *in vivo* supported that miR-223 is readily downregulated in normal mammary epithelial cells following transformation and that this downregulation could functionally contribute to tumor onset and progression. To verify if this observation could be recapitulated in the human pathology, we collected specimens from a cohort of patients with human luminal and $HER2^{+}$ breast cancer, in which areas of normal mammary tissue coexisted with areas of DCIS and IDC (Supplementary Table S2). Within each specimen, we microdissected areas of normal mammary gland tissue, DCIS, and IDC (**Fig. 6E**). Then, we extracted the RNA and quantitatively analyzed miR-223 expression by ddPCR in these three contexts. The data very clearly indicated that miR-223 levels dropped in the DCIS compared with the adjacent normal tissue and further decreased in the infiltrating breast cancer regions (**Fig. 6F**). These results were consistently maintained when matched samples from the same patient were compared (**Fig. 6G**). These findings in human samples robustly recapitulated the observation, previously collected *in vitro* and *in vivo*, that loss of miR-223 is an early event during mammary epithelial cell transformation.

Altogether, the data collected in these human samples support the possibility that loss of miR-223 expression is a potential biomarker for DCIS lesions that are likely to progress to invasive breast cancer.

Discussion

In previous work, we have investigated the cross-talk existing in patients with breast cancer between the postsurgery tumor microenvironment and the residual cancer cells (3). We found that the delivery of IORT interferes with this cross-talk, not only killing tumor cells but also altering the microenvironment at molecular level. Following IORT, miR-223 was rapidly transcribed by the mammary peritumoral tissue and, by directly targeting EGF, dampened its release during the wound-healing response, efficiently blocking the autocrine/paracrine activation of EGFR pathway in the postoperative context (3). Here, we indirectly confirmed a central role for miR-223 in the control of EGF signaling and HER2 activation, showing that miR-223 affects the activation of HER WT but not of its constitutively activated forms. Our data support the possibility of a feedback regulation that, following activation of HER2, could drive miR-223 downregulation via RB repression and E2F1 activation.

We investigated whether miR-223 could also play a role during normal mammary gland development and/or during breast tumorigenesis. *In vitro*, miR-223 regulated acinar morphogenesis of normal mammary epithelial cells grown in 3D Matrigel, and its ablation led to a partial disruption of their organization. Analyses of mammary glands from miR-223 WT female mice collected at different stages of development highlighted a striking inverse correlation between miR-223 expression levels and the developmental stage of the gland, showing a progressive downmodulation of miR-223 as the mammary epithelial cell compartment gradually expanded. However, in MMG from miR-223 KO mice, we did not observe macroscopic defects and, accordingly, these mice were able to properly lactate their litter. These results indicated that *in vivo*, under physiologic conditions, miR-223 is readily downregulated in proliferating mammary epithelial cells to allow the proper expansion of the mammary ducts necessary for a proficient lactation but also show that its loss could be compensated by other mechanisms. In the future, it will be interesting to verify if, instead, overexpression of miR-223 in normal mouse mammary gland is able to alter its postnatal development.

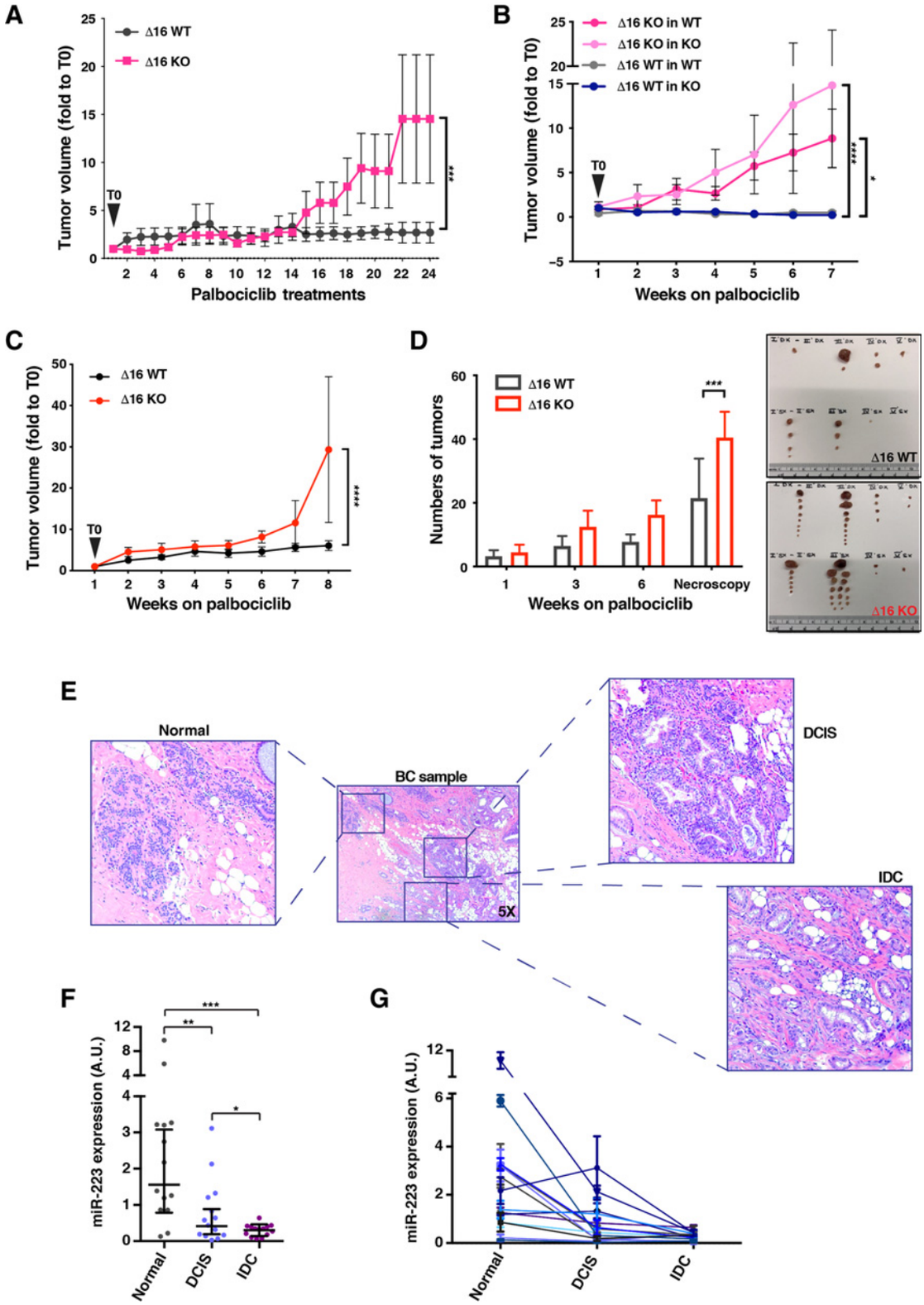

By in-depth study of the Δ16HER2 transgenic mice, we observed that the loss of miR-223 did not significantly impinge on the aggressive phenotype of this breast cancer model. Our analyses highlighted that miR-223 was no longer expressed by the cells once they become tumoral, making miR-223 WT and KO Δ16HER2 breast cancer cells essentially identical. We thus realized that, because miR-223 abrogation was a natural consequence of cell proliferation/transformation, what we needed to evaluate was the effect of its reexpression in transformed cells. Accordingly, forced overexpression of miR-223 strongly affected Δ16HER2-driven tumor cell growth, also *in vivo* (**Fig. 5**).

Many targets have been reported to mediate miR-223 effects in cell proliferation, cancer and breast cancer in particular, including Stim1 (32), and HAX (33), but none of them has demonstrated a consistent behavior in our luminal breast cancer model. We and others have reported that E2F1 and miR-223 comprise an autoregulatory negative feedback loop (12, 16). Given the involvement of E2F1 in cell cycle, it is possible that the balance of this reciprocal regulation could be critical in directing the final decision of the cell to proliferate. EGF, that we previously demonstrated as a key miR-223 target in the postsurgical tumor microenvironment (3) and that is certainly involved in mediating miR-223 effects in normal mammary epithelial cells, seems to be dispensable in the context of Δ16HER2 breast cancer model, because EGFR/HER2 pathway is already constitutively activated.

The most relevant observations of our study concern the potential translatability of our findings to the clinical setting. We find that miR-223 is downregulated in the early steps of transformation *in vitro* and *in vivo,* and DCIS lesions in patients with breast cancer dramatically lose miR-223 expression. DCIS might or not evolve in frank IDCs. Because our specimens were all from patients also IDC-positive, our selected DCIS are the ones that would likely have evolved in IDC over time. In the future, it will be interesting to verify if different expression of miR-223 correlates with clinical outcome, in patients with DCIS but not IDC, eventually allowing the use of miR-223 as a predictive biomarker of progression from DCIS to IDC.

Further, we observed that miR-223 expression increases in response to the CDK4/6 inhibitor palbociclib, *in vivo* and *in vitro*, and this increase likely represents a precocious marker of therapy efficacy. In the spontaneous FVB Δ16HER2 miR-223 WT mice, palbociclib treatment resulted not only in growth arrest of palpable tumors, but also in a dramatic decrease in the number of new tumors, whereas miR-223 KO mice continued to develop new tumors (**Fig. 6E**). This result is clinically relevant because palbociclib is administered to patients with breast cancer in the adjuvant setting, in which it acts to block the growth of disseminated tumor cells, isolated or aggregated in small foci, a situation highly reminiscent of what we observed in mice. Because miR-223 is a secreted miRNA, it would be interesting to evaluate whether miR-233 expression levels could be predictive of palbociclib response in patients with luminal breast cancer. As an alternative, it would be interesting to verify if a validated miR-223 target could serve as indirect biomarker of its expression. In many tumor types, the expression of miR-223 has been put in negative correlation with that of stathmin, an oncoprotein highly expressed in proliferating tissues, in advanced stage disease and particularly important in mammary gland development and tumorigenesis (20, 34–36). Looking at stathmin levels in correlation with those of miR-223, especially in human DCIS samples, could open new perspectives in identifying the most aggressive disease.

Here, we have focused on the connection between miR-223 and the pRB–E2F1 axis. However, because mutant p53 binds the miR-223 promoter and reduces its transcriptional activity, it will be also interesting to investigate the role and the implications of this regulatory loop in the context of mutant TP53 breast cancers (9).

Alterations of the cell cycle, eventually impinging on the pRB/E2F1 pathway, are present virtually in any human cancer. Restoring the cell-cycle control is thus one of the most intriguing ways to treat patients with many different cancers. Currently, the combined treatment with CDK4/6 inhibitors and hormonal therapy represents a successful strategy to improve prognosis of patients with luminal breast cancer. Standard of care for patients with advanced luminal breast cancer (early-stage being the next frontier) now includes a CDK4/6 inhibitors as first-line treatment (37), and the addition of CDK4/6 inhibitors to anti-HER2 therapies has proved feasible in clinical setting, with a good tolerability profile and promising efficacy (38). Thus, the need for biomarkers able to identify responders/nonresponders has become compelling. A better understanding of the factors that are involved in regulating pRB/E2F1 axis is certainly needed to identify patients that will or will not respond to those therapies, and our data indicate that miR-223 could represent a good candidate.

Overall, our work defines miR-223 downregulation as a very early event in luminal breast cancer formation and supports the possibility that it could serve as predictive biomarker of prognosis and/or response to targeted therapies that impinge on the activity of the pRB/E2F1 axis.

Figure 6.

Loss of miR-223 induces resistance to CDK4/6 inhibition and is an early marker for invasive and *in situ* ductal carcinoma. **A,** Graph reports the tumor growth of Δ16HER2 mMECs extracted from Δ16HER2 miR-223 WT and KO tumors and orthotopically and bilaterally injected in NSG mice. When tumors became palpable (T0; 10 tumors/group), mice were treated with palbociclib (100 mg/kg) 5 days/week for 5 weeks. Data are expressed as folds of tumor volume at each time point on its volume at T0, ± SEM. **B,** Graph reports the tumor growth of Δ16HER2 mMECs extracted from Δ16HER2 miR-223 WT and KO tumors, orthotopically and bilaterally injected in miR-223 WT or KO recipient mice, as indicated. When tumors became palpable (T0; 6 tumors/group), mice were treated with palbociclib (75 mg/kg) 3 days/week, for 7 weeks. Data are expressed as folds of tumor volume at each time point on its volume at T0, ± SEM. **C,** Graph reports the growth of palpable tumors in Δ16HER2 miR-223 WT and KO mice (4 mice/group) treated with palbociclib (75 mg/kg) 3 days/week for 8 weeks. Multiple tumors per mice (>5) were measured at each time point. Data are expressed as folds of tumor volume at each time point on its volume at T0, ± SEM. In all above graphs, statistical significance has been calculated by two-way ANOVA test. **D,** Graph reports the number of tumors that became palpable under palbociclib treatment and retrieved at necroscopy, in the experiment reported in **C**. Right, representative pictures of tumors extracted at necroscopy from palbociclib-treated Δ16HER2 miR-223 WT (top) and KO (bottom) mice are shown. **E,** Middle, a representative picture of hematoxylin and eosin staining of a human G3 breast cancer (BC), at ×5 magnification, is shown. In the boxes, areas of normal mammary tissue (Normal), *in situ* (DCIS), and invasive (IDC) breast cancer that were separately microdissected from each specimen are shown. **F,** Graph reports data from ddPCR analysis of normalized miR-223 expression (in arbitrary units, A.U.) in specimens from 14 patients with breast cancer containing normal mammary tissue, *in situ* (DCIS), and invasive (IDC) lesions. **G,** Graph reports the same data described in **F**, but showing which is the pattern of the three values in normal, DCIS, and IDC from each single patient. Data are expressed as normalized miR-223 median value with range. Mann–Whitney test was used for statistical analysis. Asterisks indicate significant differences. *, $P \leq 0.05$; **, $P \leq 0.01$; ***, $P \leq 0.001$; ****, $P \leq 0.0001$.

Disclosure of Potential Conflicts of Interest

No potential conflicts of interest were disclosed.

Authors' Contributions

Conception and design: F. Citron, G. Baldassarre, B. Belletti
Development of methodology: F. Citron, I. Segatto, G.L. Rampioni Vinciguerra, L. Musco, F. Russo, G. Mungo, S. D'Andrea, M.C. Mattevi
Acquisition of data (provided animals, acquired and managed patients, provided facilities, etc.): T. Perin, M. Schiappacassi, S. Massarut, C. Marchini, A. Amici, A. Vecchione, B. Belletti
Analysis and interpretation of data (e.g., statistical analysis, biostatistics, computational analysis): F. Citron, A. Vecchione, G. Baldassarre, B. Belletti
Writing, review, and/or revision of the manuscript: F. Citron, G. Baldassarre, B. Belletti
Administrative, technical, or material support (i.e., reporting or organizing data, constructing databases): F. Citron, I. Segatto, G.L. Rampioni Vinciguerra
Study supervision: G. Baldassarre, B. Belletti

Acknowledgments

We like to thank all patients who have donated their tissue and made our research possible. We also like to thank all the staff of the Pathology Unit for their valuable technical support; present and past members of the S.C.I.C.C. lab for valuable contributions; and all members of the Molecular Oncology Unit for critical discussion of the data.

This work was supported by the Associazione Italiana per la Ricerca sul Cancro (AIRC) to B. Belletti (IG 20061); by CRO Intramural Research Grant (5 × 1000_2016_MdS) to I. Segatto; by *L.R. 17*/2014-Regione FVG (TuMaGiDo and TNBCNeo) to G. Baldassarre; and by Associazione Italiana per la Ricerca sul Cancro (AIRC fellowships) to I. Segatto (#18171) and F. Citron (#20902).

The costs of publication of this article were defrayed in part by the payment of page charges. This article must therefore be hereby marked *advertisement* in accordance with 18 U.S.C. Section 1734 solely to indicate this fact.

Received June 13, 2019; revised November 19, 2019; accepted December 17, 2019; published first December 20, 2019.

References

1. Dragomir M, Mafra ACP, Dias SMG, Vasilescu C, Calin GA. Using microRNA networks to understand cancer. Int J Mol Sci 2018;19.
2. Shah MY, Ferrajoli A, Sood AK, Lopez-Berestein G, Calin GA. microRNA therapeutics in cancer - an emerging concept. EBioMedicine 2016;12: 34–42.
3. Fabris L, Berton S, Citron F, D'Andrea S, Segatto I, Nicoloso MS, et al. Radiotherapy-induced miR-223 prevents relapse of breast cancer by targeting the EGF pathway. Oncogene 2016;35:4914–26.
4. Vaidya JS, Wenz F, Bulsara M, Tobias JS, Joseph DJ, Keshtgar M, et al. Risk-adapted targeted intraoperative radiotherapy versus whole-breast radiotherapy for breast cancer: 5-year results for local control and overall survival from the TARGIT-A randomised trial. Lancet 2014;383:603–13.
5. Vaidya JS, Joseph DJ, Tobias JS, Bulsara M, Wenz F, Saunders C, et al. Targeted intraoperative radiotherapy versus whole breast radiotherapy for breast cancer (TARGIT-A trial): an international, prospective, randomised, non-inferiority phase 3 trial. Lancet 2010;376:91–102.
6. Johnnidis JB, Harris MH, Wheeler RT, Stehling-Sun S, Lam MH, Kirak O, et al. Regulation of progenitor cell proliferation and granulocyte function by microRNA-223. Nature 2008;451:1125–9.
7. O'Connell RM, Zhao JL, Rao DS. MicroRNA function in myeloid biology. Blood 2011;118:2960–9.
8. Jeffries J, Zhou W, Hsu AY, Deng Q. miRNA-223 at the crossroads of inflammation and cancer. Cancer Lett 2019;451:136–41.
9. Masciarelli S, Fontemaggi G, Di Agostino S, Donzelli S, Carcarino E, Strano S, et al. Gain-of-function mutant p53 downregulates miR-223 contributing to chemoresistance of cultured tumor cells. Oncogene 2014;33:1601–8.
10. Dong Z, Qi R, Guo X, Zhao X, Li Y, Zeng Z, et al. MiR-223 modulates hepatocellular carcinoma cell proliferation through promoting apoptosis via the Rab1-mediated mTOR activation. Biochem Biophys Res Commun 2017;483: 630–7.
11. Pinatel EM, Orso F, Penna E, Cimino D, Elia AR, Circosta P, et al. miR-223 is a coordinator of breast cancer progression as revealed by bioinformatics predictions. PloS One 2014;9:e84859.
12. Pulikkan JA, Dengler V, Peramangalam PS, Peer Zada AA, Müller-Tidow C, Bohlander SK, et al. Cell-cycle regulator E2F1 and microRNA-223 comprise an autoregulatory negative feedback loop in acute myeloid leukemia. Blood 2010; 115:1768–78.
13. Stamatopoulos B, Meuleman N, Haibe-Kains B, Saussoy P, Van Den Neste E, Michaux L, et al. microRNA-29c and microRNA-223 down-regulation has in vivo significance in chronic lymphocytic leukemia and improves disease risk stratification. Blood 2009;113:5237–45.
14. Fassan M, Saraggi D, Balsamo L, Realdon S, Scarpa M, Castoro C, et al. Early miR-223 upregulation in gastroesophageal carcinogenesis. Am J Clin Pathol 2017;147:301–8.
15. Streppel MM, Pai S, Campbell NR, Hu C, Yabuuchi S, Canto MI, et al. microRNA 223 is upregulated in the multistep progression of barrett9s esophagus and modulates sensitivity to chemotherapy by targeting PARP1. Clin Cancer Res 2013;19:4067–78.
16. Armenia J, Fabris L, Lovat F, Berton S, Segatto I, D'Andrea S, et al. Contact inhibition modulates intracellular levels of miR-223 in a p27kip1-dependent manner. Oncotarget 2014;5:1185–97.
17. Barrio AV, Van Zee KJ. Controversies in the treatment of DCIS. Annu Rev Med 2017;68:197–211.
18. Marchini C, Gabrielli F, Iezzi M, Zenobi S, Montani M, Pietrella L, et al. The human splice variant Δ16HER2 induces rapid tumor onset in a reporter transgenic mouse. PloS One 2011;6:e18727.
19. Ince TA, Richardson AL, Bell GW, Saitoh M, Godar S, Karnoub AE, et al. Transformation of different human breast epithelial cell types leads to distinct tumor phenotypes. Cancer Cell 2007;12:160–70.
20. Segatto I, Zompit MDM, Citron F, D'Andrea S, Vinciguerra GLR, Perin T, et al. Stathmin is required for normal mouse mammary gland development and delta16HER2-driven tumorigenesis. Cancer Res 2019; 79:397–409.
21. Bakin AV, Tomlinson AK, Bhowmick NA, Moses HL, Arteaga CL. Phosphatidylinositol 3-kinase function is required for transforming growth factor beta-mediated epithelial to mesenchymal transition and cell migration. J Biol Chem 2000;275:36803–10.
22. Fabris L, Berton S, Pellizzari I, Segatto I, D'Andrea S, Armenia J, et al. p27kip1 controls H-Ras/MAPK activation and cell cycle entry via modulation of MT stability. Proc Natl Acad Sci 2015;112:13916–21.
23. Sonego M, Schiappacassi M, Lovisa S, Dall'Acqua A, Bagnoli M, Lovat F, et al. Stathmin regulates mutant p53 stability and transcriptional activity in ovarian cancer. EMBO Mol Med 2013;5:707–22.
24. Segatto I, Berton S, Sonego M, Massarut S, D'Andrea S, Perin T, et al. Inhibition of breast cancer local relapse by targeting p70S6 kinase activity. J Mol Cell Biol 2013;5:428–31.
25. Segatto I, Berton S, Sonego M, Massarut S, Fabris L, Armenia J, et al. p70S6 kinase mediates breast cancer cell survival in response to surgical wound fluid stimulation. Mol Oncol 2014;8:766–80.
26. Dall'Acqua A, Sonego M, Pellizzari I, Pellarin I, Canzonieri V, D'Andrea S, et al. CDK6 protects epithelial ovarian cancer from platinum-induced death via FOXO3 regulation. EMBO Mol Med 2017;9:1415–33.
27. Berton S, Pellizzari I, Fabris L, D'Andrea S, Segatto I, Canzonieri V, et al. Genetic characterization of p27kip1 and stathmin in controlling cell proliferation in vivo. Cell Cycle 2014;13:3100–11.
28. Citron F, Armenia J, Franchin G, Polesel J, Talamini R, D'Andrea S, et al. An integrated approach identifies mediators of local recurrence in head and neck squamous carcinoma. Clin Cancer Res 2017;23:3769–80.
29. Nagy Á, Lánczky A, Menyhárt O, Győrffy B. Validation of miRNA prognostic power in hepatocellular carcinoma using expression data of independent datasets. Sci Rep 2018;8:9227.
30. Kwong KY, Hung MC.A novel splice variant of HER2 with increased transformation activity. Mol Carcinog 1998;23:62–8.
31. Serra V, Vivancos A, Puente XS, Felip E, Silberschmidt D, Caratu G, et al. Clinical response to a lapatinib-based therapy for a Li-Fraumeni syndrome patient with a novel HER2V659E mutation. Cancer Discov 2013;3:1238–44.

32. Yang Y, Jiang Z, Ma N, Wang B, Liu J, Zhang L, et al. MicroRNA-223 targeting STIM1 inhibits the biological behavior of breast cancer. Cell Physiol Biochem 2018;45:856–66.
33. Sun X, Li Y, Zheng M, Zuo W, Zheng W. MicroRNA-223 increases the sensitivity of triple-negative breast cancer stem cells to TRAIL-induced apoptosis by targeting HAX-1. PloS One 2016;11:e0162754.
34. Kang W, Tong JHM, Chan AWH, Lung RWM, Chau SL, Wong QWL, et al. Stathmin1 plays oncogenic role and is a target of microRNA-223 in gastric cancer. PloS One 2012;7:e33919.
35. Imura S, Yamada S, Saito YU, Iwahashi S, Arakawa Y, Ikemoto T, et al. miR-223 and stathmin-1 expression in non-tumor liver tissue of patients with hepatocellular carcinoma. Anticancer Res 2017;37:5877–83.
36. Wong QW-L, Lung RW-M, Law PT-Y, Lai PB-S, Chan KY-Y, To K-F, et al. MicroRNA-223 is commonly repressed in hepatocellular carcinoma and potentiates expression of Stathmin1. Gastroenterology 2008;135:257–69.
37. Im S-A, Lu Y-S, Bardia A, Harbeck N, Colleoni M, Franke F, et al. Overall survival with ribociclib plus endocrine therapy in breast cancer. N Engl J Med 2019;381:307–16.
38. Gianni L, Bisagni G, Colleoni M, Del Mastro L, Zamagni C, Mansutti M, et al. Neoadjuvant treatment with trastuzumab and pertuzumab plus palbociclib and fulvestrant in HER2-positive, ER-positive breast cancer (NA-PHER2): an exploratory, open-label, phase 2 study. Lancet Oncol 2018;19:249–56.